Journal of Sound and Vibration (2002) **252**(1), 65–82
doi:10.1006/jsvi.2001.4026, available online at http://www.idealibrary.com on IDEAL®

AN INVERSE METHOD TO COMPUTE EQUIVALENT FORCES ON A STRUCTURE BASED ON SOUND POWER MEASUREMENTS

M. Y. Yang and G. H. Koopmann

Noise Control Laboratory, Center for Acoustics and Vibration, The Pennsylvania State University, 157 Hammond Building, University Park, PA 16802, *U.S.A.*

(*Received* 18 *December* 2000, *and in final form* 14 *September* 2001)

When modelling the dynamic response of an existing structure to predict the effects of design modifications, many types of forces are difficult to characterize, e.g., those due to unsteady flows or acoustic excitation. To model the forcing function in such cases, a method is presented which solves for an equivalent forcing function based on sound power measurements. The method assumes that the equivalent forcing function may be represented with a superposition of force distributions on a mode-by-mode basis, i.e., there is one force distribution per eigenvalue with the shape of the eigenvector. The method is applied to cases where the structure is lightly damped and has low modal density. Experimental results show that the method accurately predicts the effect of design changes on the structure's radiated sound power. The accuracy of the method is sensitive to small differences between the experimental and theoretical natural frequencies and thus it is important to match the damped natural frequencies of the physical structure as accurately as possible.

1. INTRODUCTION

Optimization techniques are an increasingly popular tool for applying noise and vibration control treatments to existing structures. One method is to first model the structure in terms of its eigenmodes (obtained either experimentally or numerically) and then use an optimization search to introduce changes in the design that minimize a response parameter, say sound power radiation [1]. Difficulties often arise, however, when attempting to characterize the forcing function required by the optimization routine. This is particularly true in cases where the structure's response is due to acoustic excitation or flow-induced noise as in the case of say, the fuselage skin of an airplane. One common approach that falls in the category of inverse problems is to measure the response of the structure within the bandwidth of interest and then solve for an equivalent forcing function that gives the same response. In the case where design modifications are anticipated, not only must the equivalent force duplicate the original response of the structure, but it must also accurately predict the effects of the structural modifications.

Experimentalists typically formulate the inverse problem by measuring the surface response at discrete points and inversely solving for the force by modelling the structure in some form of a modal expansion. This method works reasonably well for structures with simple geometries and low wavenumber modes. However, for structures with more complex geometries and higher wavenumber modes, the number of measurement points required to converge to a stable inverse solution becomes unrealistically large.

0022-460X/02/$35.00

For flow-induced forcing functions, several researchers have attempted to characterize the pressure on a surface excited with a turbulent boundary layer (TBL). These methods are largely statistical in nature. Maidanik and Jorgenson [2] have described a method whereby the spectral density of the TBL can be directly measured as a function of wavenumber and frequency. This method is primarily used for the low-wavenumber region. A few measurements have been reported based on their method [3–5]. Hwang and Geib [6] use a regression approach to expand the estimation of TBL excitation to the entire wavenumber spectrum.

Fulford and Gibbs [7–9] attempted to characterize dynamic sources with respect to "vibrational power". They used two functions, the source descriptor [10] and the coupling function to establish the power delivered by the source. Both analytical and statistical studies were performed, with only the statistical study providing reliable results.

Much effort has been directed to the discrete inverse problem in acoustics, wherein the acoustic source strengths are deduced from measured acoustic pressures by inversion of a matrix of transfer functions. One approach is the use of nearfield acoustic holography (NAH), first introduced by Maynard *et al.* [11]. Veronesi and Maynard [12] later described the implementation of NAH. Grace *et al.* [13, 14] have studied the aeroacoustic inverse problem of characterizing the unsteady surface pressures along a streamlined airfoil from the measurement of the radiated sound field. A good summary of the possibilities and limitations of the use of inverse methods is given by Nelson and Yoon [15]. They later augmented the inverse methods with two regularization methods [16] (Tikhonov regularization and singular value discarding) to reconstruct the volume velocities of a simply supported vibrating plate.

Craun and Feit [17] combined the use of pseudo-inverse and matched-field processing methods to characterize the broadband random vibration source on a lightly damped frame structure. The authors state that the method has several weaknesses, including the requirement of a large number of observed response points, and the importance of sensor placement.

The motivation behind the work presented in this paper was to develop a method that is straightforward to implement for a designer wanting to add modifications to a structure to reduce its noise and/or vibration. Measuring radiated sound power instead of a structure's surface vibration enables many measurement difficulties to be circumvented. These include, for example, the need for a steady phase reference, measurements on complex-shaped surfaces or coherence problems that arise from unsteady forces due to say, internal combustion processes. All of these problems are usually encountered if the vibrating surface of a structure is measured with conventional instrumentation such as scanning laser vibrometers or accelerometers.

It should be noted however, that the inverse solution method becomes somewhat more complicated when the force is computed from a sound power measurement since the interaction between the vibrating structure and the surrounding fluid must also be modelled. However, as we show in this paper, this modelling complication is balanced by the straightforward manner in which sound power is related to the surface velocity of the structure through an acoustic resistance matrix, a quantity generated by a lumped parameter, boundary element method.

2. MATHEMATICAL FORMULATION

2.1. DYNAMIC RESPONSE OF THE STRUCTURE

Using the expansion theorem, the dynamic response of a structure is written as the summation of basis each multiplied by some constant. We often choose the eigenvectors of

the structure as the basis shapes out of convenience since these are obtained either from modal analysis experiments on the physical structure or finite elements models. This is written as

$$\mathbf{x} = \sum_{n=1}^{N} y_n \boldsymbol{\psi}_n = \boldsymbol{\Phi}\mathbf{y}, \tag{1}$$

where $\mathbf{x}$ is the vector of displacements, y_n is the *modal participation factor*, $\boldsymbol{\Psi}_n$ is the nth eigenvector, and $\boldsymbol{\Phi}$ is the modal matrix, with the eigenvectors in columns.

The modal participation factor can be written as

$$y_n = \sum_{\mu'} \frac{\boldsymbol{\psi}_n(\mu')F(\mu')}{\omega_{d_n}^2 - \omega^2}, \tag{2}$$

where $F(\mu')$ is the force at the center of a single element, $\omega_{d_n}^2 = \omega_n^2(1 + \mathrm{i}\eta_n)$ is the nth damped natural frequency, and η_n is the modal loss factor.

In our inverse method, we divide the existing structure into multiple nodes that surround planar elemental surfaces. The eigenvectors are measured directly or computed using a finite element model. In either case, the space-average velocity *normal* to *each element* is measured or calculated, since this is the quantity required as input to the acoustic boundary element program. In the finite element model the rotary terms and the eigenvector components tangential to the surface are neglected because they contribute little to sound radiation. Orthogonally still applies since the tangential terms are much smaller than the normal terms.

The sound power calculation requires knowledge of the volume velocity, $u(\mu)$, at each elemental surface. This is found by substituting equation (2) into equation (1), and multiplying by $\mathrm{i}\omega$ and the elemental surface area S_μ:

$$u(\mu) = \mathrm{i}\omega S_\mu \sum_{n=1}^{N} \boldsymbol{\psi}_n(\mu) \sum_{\mu'} \frac{\boldsymbol{\psi}_n(\mu')F(\mu')}{\omega_{d_n}^2 - \omega^2} \tag{3}$$

or

$$\mathbf{u} = \mathrm{i}\omega\mathbf{A}\boldsymbol{\Phi}\boldsymbol{\Omega}\boldsymbol{\Phi}^{\mathrm{T}}\mathbf{f}, \tag{3a}$$

where $\mathbf{f}$ is the column vector of force magnitudes and phases, $\mathbf{A}$ is the diagonal matrix of elemental areas, and $\boldsymbol{\Omega}$ is another diagonal matrix:

$$\Omega_{ij} = \frac{1}{\omega_{d_i}^2 - \omega^2} \quad \text{for } i = j,$$
$$\Omega_{ij} = 0 \quad \text{for } i \neq j, \tag{4}$$

$$A_{ij} = S_\mu \quad \text{for } i = j,$$
$$A_{ij} = 0 \quad \text{for } i \neq j. \tag{5}$$

2.2. THE ADDITION OF CONTROL IMPEDANCES

To illustrate our design method that motivated the need for an equivalent force computation, we choose a few simple examples wherein the structural modifications are

modelled as point impedances (e.g., lumped masses or tuned vibration absorbers; thus the impedance matrix is diagonal). The point impedance for a lumped mass is

$$Z_{mass} = \mathrm{i}\omega m_{mass}, \tag{6}$$

while for a tuned absorber, the point impedance is

$$Z_{TVA} = \mathrm{i}\omega \frac{m_{TVA}k_{TVA}(1 + \mathrm{i}\eta_{TVA})}{k_{TVA}(1 + \mathrm{i}\eta_{TVA}) - \omega^2}, \tag{7}$$

where m_{mass} is the mass of the lumped mass, m_{TVA} is the mass of the tuned vibration absorber, k_{TVA} is the equivalent stiffness of the tuned vibration absorber, and η_{TVA} is the equivalent loss factor of the tuned vibration absorber.

Note that if a multi-point impedance is used (e.g., a stiffening rib), the impedance matrix will no longer be diagonal.

Introducing the design modifications as external forces is a significant time-saving step in the optimization process since it circumvents the need to generate a new eigenvector solution with each modification. For large, complex structures, this is a computationally expensive and time-consuming process.

The mobility $\mathbf{Y}$ of the structure can be derived with the definition of mobility and equation (3a). The vector of velocities $\mathbf{v}$ is

$$\mathbf{v} = \mathbf{A}^{-1}\mathbf{u} = \mathbf{Y}\mathbf{f} = \mathrm{i}\omega\mathbf{\Phi\Omega\Phi}^{\mathrm{T}}\mathbf{f}. \tag{8}$$

This gives the structure mobility

$$\mathbf{Y} = \mathrm{i}\omega\mathbf{\Phi\Omega\Phi}^{\mathrm{T}}. \tag{9}$$

The final volume velocity of the structure with control impedances is now

$$\mathbf{u} = \mathbf{A}(\mathbf{I} + \mathbf{YZ})^{-1}\mathbf{Y}\mathbf{f}, \tag{10}$$

where $\mathbf{I}$ is an $N \times N$ identity matrix, and $\mathbf{Z}$ is the control impedance matrix. Equation (10) is derived by writing the velocity at each point in terms of the forces (from the control impedances) and the mobilities of the structure. It is derived in greater detail by Constans [18]. Note that if there are no control impedances, $\mathbf{Z}$ is a zero matrix and equation (10) will be identical to equation (3a).

2.3. GENERALIZED FORCE SOLUTION/USING MODE SHAPED FORCES

We start by choosing N different force distributions, one for each eigenvector. Each force distribution covers the entire surface of the radiating structure and has the *same spatial distribution* as its corresponding eigenvector. This will eventually enable us to use orthogonality, which allows each force distribution to affect only its corresponding eigenmode.

The total force F_T acting on the surface is the superposition of the N force distributions:

$$F_T(\omega, \mu') = \sum_{m=1}^{N} f_m(\omega)\mathrm{e}^{\mathrm{i}\phi_m(\omega)}\phi_n(\mu'), \tag{11}$$

where f_m and ϕ_m are the magnitude and phase of each force distribution respectively. Note that equation (11) can also be written in matrix form as

$$\mathbf{F} = \mathbf{\Phi f}. \tag{11a}$$

We recognize equation (11a) to be the *generalized force* and substituting it into equation (3) yields

$$u(\mu) = \mathrm{i}\omega S_\mu \sum_{n=1}^{N} \frac{\boldsymbol{\psi}_n(\mu)}{\omega_{d_n}^2 - \omega^2} \sum_{m=1}^{N} f_m \mathrm{e}^{\mathrm{i}\phi_m} \sum_{\mu'} \boldsymbol{\psi}_m(\mu')\boldsymbol{\psi}_n(\mu'). \tag{12}$$

Due to orthogonality, the last summation term will equal zero for $n \neq m$.

For the case where $n = m$, the expression becomes

$$u(\mu) = \mathrm{i}\omega S_\mu \sum_{n=1}^{N} \frac{\boldsymbol{\psi}_n(\mu)}{\omega_{d_n}^2 - \omega^2} f_n \mathrm{e}^{\mathrm{i}\phi_n} \sum_{\mu'} \boldsymbol{\psi}_n^2(\mu'). \tag{12a}$$

Note how the force magnitude and phase have been effectively isolated from the other terms. This will be important when we attempt to solve for the force.

Adding control impedances in the same manner as equation (10) and rewriting it in matrix form gives

$$\mathbf{u} = \mathbf{\Lambda f}, \tag{13}$$

where

$$\mathbf{\Lambda} = \mathbf{A}(\mathbf{I} + \mathbf{YZ})^{-1}\mathbf{Y\Phi}. \tag{14}$$

We are now at a point where the volume velocity can be combined with the acoustic resistance to give the radiated sound power. The expression for radiated sound power in matrix form is

$$\Pi = \tfrac{1}{2}\mathbf{u}^{\mathrm{H}}\mathbf{Ru}, \tag{15}$$

where H is the Hermitian (complex conjugate transpose), and **R** is the radiation resistance matrix. In this study, the terms in the matrix **R** are calculated over the frequency range of interest prior to the optimization process and are stored in a formatted file. (See Appendix A for details regarding the calculation of **R**.)

Substituting equation (13) into equation (15) yields

$$\Pi = \tfrac{1}{2}\mathbf{f}^{\mathrm{H}}\mathbf{\Lambda}^{\mathrm{H}}\mathbf{R\Lambda f}. \tag{16}$$

At this point, it is difficult to explicitly solve for the force vectors, **f**, since they appear at the beginning and end of three full matrices. Any further attempt must address the cross terms that appear as

$$(f_m \mathrm{e}^{-\mathrm{i}\phi_m})(f_n \mathrm{e}^{\mathrm{i}\phi_n}), \quad \text{where} \quad m \neq n. \tag{17}$$

2.4. ELIMINATING THE CROSS TERMS

To simplify the analysis, let the impedance matrix **Z** be a null matrix (no control impedances), and assume that **A** = identity. By combining equations (9), (14), and (16), the

expression for power simplifies to

$$\Pi = \tfrac{1}{2}\mathbf{f}^{\mathrm{H}}\mathbf{\Omega}^{*}\mathbf{Y}^{\mathrm{H}}\mathbf{\Phi}^{\mathrm{T}}\mathbf{R}\mathbf{Y}\mathbf{\Phi}\mathbf{\Omega}\mathbf{f}. \tag{18}$$

We will further assume that the dominant terms in equation (18) are the frequency terms in $\mathbf{\Omega}$ and examine their product, $\mathbf{W} = \mathbf{\Omega}^{*}\mathbf{\Omega}$, in greater detail. Recall that $\mathbf{\Omega}$ is a diagonal matrix. Each individual term of the product appears as

$$W_{mn} = \frac{1}{\omega_m^2(1 - \mathrm{i}\eta_m) - \omega^2}\,\frac{1}{\omega_n^2(1 + \mathrm{i}\eta_n) - \omega^2}, \tag{19}$$

where ω_m and ω_n are the mth and nth natural frequencies respectively.

2.4.1. *Direct terms*

First, consider the direct terms ($n = m$):

$$W = \frac{1}{\omega_n^4(1 + \eta_n^2) - 2\omega_n^2\omega^2 + \omega^4}. \tag{20}$$

For $\omega = \omega_n$ (at resonance):

$$W = \frac{1}{\omega_n^4\eta_n^2}. \tag{21a}$$

For $\omega \ll \omega_m$ (below lowest resonance):

$$W = \frac{1}{\omega_n^4(1 + \eta_n^2)}. \tag{21b}$$

For $\omega \gg \omega_n$ (above highest resonance):

$$W = \frac{1}{\omega^4}, \tag{21c}$$

2.4.2. *Cross terms*

To examine the cross terms, assume that ω_m and ω_n can be related through the relationship

$$\omega_n = r\omega_m, \quad \text{where} \quad r > 1. \tag{22}$$

Further, assume that $\eta_m = \eta_n = \eta$ and that η is small.

For the case where $\omega = \omega_m$ (at lower resonance):

$$W = \frac{1}{-\mathrm{i}\eta r^2\omega_m^4 + r^2\omega_m^4\eta^2 + \mathrm{i}\eta\omega_m^4}. \tag{23a}$$

For the case where $\omega = \omega_n$ (at higher resonance):

$$W = \frac{1}{\mathrm{i}\eta r^2\omega_m^4(1 - r^2 - \mathrm{i}\eta)}. \tag{23b}$$

For the case where $\omega = 1/2\ (\omega_m + \omega_n)$:

$$W = \frac{1}{\omega_m^4\left[\left(\frac{3}{4} - \frac{1}{2}r - \frac{1}{4}r^2\right) - \mathrm{i}\eta\right]\left[\left(\frac{1}{4} - \frac{1}{2}r + \frac{3}{4}r^2\right) + \mathrm{i}r^2\eta\right]}. \tag{23c}$$

For the case where $\omega \ll \omega_m$ (below lowest resonance):

$$W = \frac{1}{r^2 \omega_m^4 (1 + \eta^2)}. \tag{23d}$$

For the case where $\omega \gg \omega_n$ (above highest resonance):

$$W = \frac{1}{\omega^4}. \tag{23e}$$

2.4.3. *Ratio of cross- and direct-terms*

The ratio of the cross/direct terms can now be taken by dividing the results in equations (23a–e) by the results in equations (21a–c). If the absolute magnitude of the resulting ratio is small, then the cross terms can be considered negligible in relation to the direct terms.

First, consider the case where the evaluation occurs at the lower resonance. The ratio is found by dividing equation (23a) by (21a):

$$\frac{CrossTerm}{DirectTerm} = \frac{\eta}{\mathrm{i}(1 - r^2 - \mathrm{i}r^2\eta)}. \tag{24a}$$

For the case where the evaluation occurs at the higher resonance, divide equation (23b) by (21a):

$$\frac{CrossTerm}{DirectTerm} = \frac{\eta}{\mathrm{i}r^2(1 - r^2 - \mathrm{i}\eta)}. \tag{24b}$$

For the case where the evaluation occurs midway between the two resonances, divide equation (23c) by (21a):

$$\frac{CrossTerm}{DirectTerm} = \frac{\eta^2}{\left[\frac{3}{4} - \frac{1}{2}r - \frac{1}{4}r^2 - \mathrm{i}\eta\right]\left[-\frac{1}{4} - \frac{1}{2}r + \frac{3}{4}r^2 + \mathrm{i}r^2\eta\right]}. \tag{24c}$$

For the case where the evaluation occurs below the lowest resonance, divide equation (23d) by (21b):

$$\frac{CrossTerm}{DirectTerm} = \frac{1}{r^2}. \tag{24d}$$

For the case where the evaluation occurs above the highest resonance, divide equation (23e) by (21c):

$$\frac{CrossTerm}{DirectTerm} = 1. \tag{24e}$$

Figure 1 plots the cross/direct term ratio for the different cases. It is apparent that the ratio is sufficiently small provided the separation between resonances is large enough, and the frequency of evaluation is between the lowest and highest resonance frequencies. Figure 2 shows that as the loss factor increases, the modal separation also needs to increase. For the example used in this study to illustrate the method, from this point on, we will assume that the modal separation is high enough and the loss factor low enough such that the cross terms are negligible.

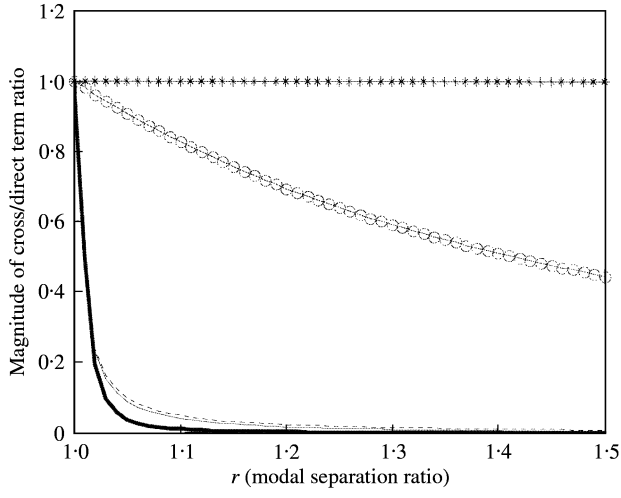

Figure 1. Cross/direct term ratio versus modal separation. Loss factor = 0·01; - - - -, lower resonance; ——, higher resonance; ▬▬, mid resonance; ○, below lowest resonance; −∗−, above highest resonance.

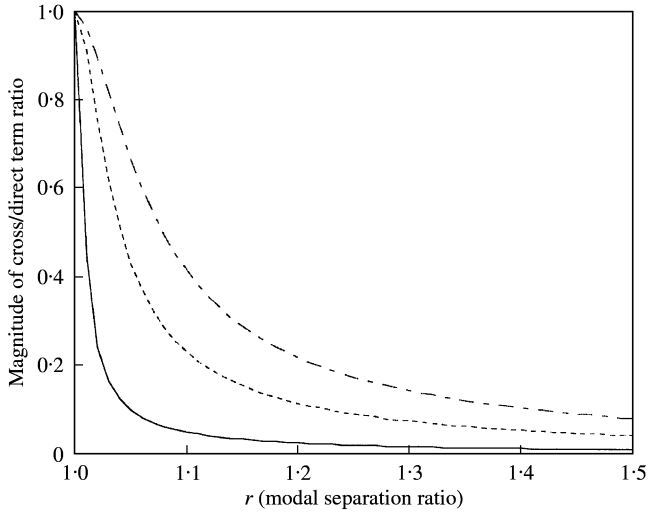

Figure 2. Effect of loss factor on cross/direct term ratio: — - —, loss factor = 0·01; - - - -, loss factor = 0·05; ——, loss factor = 0·10.

2.5. SOLVING FOR FORCE WITH CROSS TERMS NEGLIGIBLE

It can be shown that if the cross terms are negligible, equation (18) becomes

$$\Pi = \frac{1}{2}\sum_{n=1}^{N}(f_n e^{i\phi_n})(f_n e^{i\phi_n})^*\,[\Lambda_{1n}\ \Lambda_{2n}\ \cdots\ \Lambda_{\mu n}]^*[\mathbf{R}]\begin{bmatrix}\Lambda_{1n}\\ \Lambda_{2n}\\ \vdots\\ \Lambda_{\mu n}\end{bmatrix}, \tag{25}$$

where $\Lambda_{1n}, \Lambda_{2n} \ldots \Lambda_{\mu n}$, is a single column of the $\mathbf{\Lambda}$ matrix (see equation (14)). Note that the complex conjugate will cause the phase terms of the generalized force f_n to cancel. Now only the magnitude of the force will need to be determined.

The problem will now be simplified further by assuming that the generalized force is *not a function of frequency*. This is a valid assumption because we are effectively solving for the contribution of each mode to the total radiated sound power. Each mode radiates highest at its resonance frequency, and sound radiation at other frequencies (for lightly damped structures) is negligible in comparison. By keeping the generalized forces constant with respect to frequency, we are effectively neglecting the contribution of the mode away from its resonance. This allows us to express the sound power at K frequencies as

$$\begin{Bmatrix} \Pi(\omega_1) \\ \Pi(\omega_2) \\ \vdots \\ \Pi(\omega_K) \end{Bmatrix} = \frac{1}{2} \begin{bmatrix} \gamma \\ K \times N \end{bmatrix} \begin{Bmatrix} |f_1|^2 \\ |f_2|^2 \\ \vdots \\ |f_N|^2 \end{Bmatrix}, \tag{26}$$

where γ is a function of n and ω, and each term is defined as

$$\gamma_{kn} = [\Lambda_{1n} \;\; \Lambda_{2n} \;\; \cdots \;\; \Lambda_{\mu n}]^* [\mathbf{R}] \begin{bmatrix} \Lambda_{1n} \\ \Lambda_{2n} \\ \vdots \\ \Lambda_{\mu n} \end{bmatrix}. \tag{27}$$

It is important to remember that both $\mathbf{\Lambda}$ and $\mathbf{R}$ are functions of frequency.

The equivalent force can be solved with equation (26). If there is an equivalent number of modes and frequencies ($N = K$), a direct matrix inversion is used to solve for the generalized force. If there are a greater number of modes than frequencies ($N > K$), a numerical method such as singular value decomposition can be used. If there are a fewer number of modes than frequencies ($N < K$), the problem is under-specified and a unique solution is not possible.

2.6. RECALCULATING STRUCTURE RESPONSE USING CONTROL IMPEDANCES

Once the equivalent forces have been found, the response of the structure when modified with control impedances (masses, TVA's, etc.) can be calculated in a straightforward manner. To illustrate this procedure, we begin by stating that the base structure is influenced by both external forces $\mathbf{F}$, and by forces from the control impedances, $\mathbf{e}$. The velocity of the structure, $\mathbf{v}$, can be written as

$$\mathbf{v} = \mathbf{Y}(\mathbf{F} - \mathbf{e}) = \mathbf{YF} - \mathbf{Ye}. \tag{28}$$

We can split the velocity vector into two parts: velocities at locations where control impedances exist, $\mathbf{v}_a$, and velocities at all other locations, $\mathbf{v}_b$. The same can be done for the mobility and force matrices. In all cases, the subscript a indicates locations with control impedances, and the subscript b indicates all other locations.

$$\begin{Bmatrix} \mathbf{v}_a \\ \mathbf{v}_b \end{Bmatrix} = \begin{bmatrix} \mathbf{Y}_{aa} & \mathbf{Y}_{ab} \\ \mathbf{Y}_{ba} & \mathbf{Y}_{bb} \end{bmatrix} \begin{Bmatrix} \mathbf{F}_a \\ \mathbf{F}_b \end{Bmatrix} - \begin{bmatrix} \mathbf{Y}_{aa} & \mathbf{Y}_{ab} \\ \mathbf{Y}_{ba} & \mathbf{Y}_{bb} \end{bmatrix} \begin{Bmatrix} \mathbf{e} \\ \mathbf{0} \end{Bmatrix}. \tag{29}$$

The two velocity vectors are solved independently:

$$\mathbf{v}_a = \mathbf{Y}_{aa}\mathbf{F}_a + \mathbf{Y}_{ab}\mathbf{F}_b - \mathbf{Y}_{aa}\mathbf{e}, \tag{30}$$

$$\mathbf{v}_b = \mathbf{Y}_{ba}\mathbf{F}_a + \mathbf{Y}_{bb}\mathbf{F}_b - \mathbf{Y}_{ba}\mathbf{e}. \tag{31}$$

The impedance force is written

$$\mathbf{e} = \mathbf{Z}_{aa}\mathbf{v}_a, \tag{32}$$

where $\mathbf{Z}_{aa}$ is the $p \times p$ matrix of control impedances, p being the number of points affected by the impedances.

By using mode-shaped forces ($\mathbf{F} = \mathbf{\Phi f}$) and multiplying the velocities by elemental areas to obtain volume velocity, we get

$$\mathbf{u}_a = \mathbf{A}(\mathbf{I} + \mathbf{Y}_{aa}\mathbf{Z}_{aa})^{-1}[\mathbf{Y}_{aa} \;\; \mathbf{Y}_{ab}](\mathbf{\Phi f}), \tag{33}$$

$$\mathbf{u}_b = \mathbf{A}[\mathbf{Y}_{ba} \;\; \mathbf{Y}_{bb}](\mathbf{\Phi f}) - \mathbf{Y}_{ba}(\mathbf{Z}_{aa}\mathbf{u}_a). \tag{34}$$

The advantage of this method should now be apparent. Each time modifications are made to the structure, only a small $p \times p$ matrix needs to be inverted. Traditional methods that used the finite element method to recalculate the structure's response required the solution of very large matrices, a very time-consuming process. By using equation (26) to solve for a generalized force, and then using equations (33) and (34) to calculate the response, we have now made optimization methods requiring many iterations feasible.

3. PROCEDURE SUMMARY

Since many steps are required, the following summarizes how an equivalent force is determined for an existing structure.

(1) Begin by measuring the sound power spectrum radiated by the structure over the frequency range of interest at typical operating conditions.
(2) Conduct a modal analysis of the existing structure either experimentally or via the finite element method. Typical loss factors should be measured when possible.
(3) Compute the normal component of the eigenvector at each element along with its corresponding volume velocity (rotary degrees of freedom are assumed negligible).
(4) Evaluate the resistance matrix over frequency range of interest. For example, this can be done using the program POWER (see reference [3]). Note: The resistance matrix varies slowly with frequency at the low- to mid-frequency range ($ka < 2$). Therefore, it is possible to speed up the computation process by interpolating the resistance matrix, say every 5 Hz.
(5) Use equation (26) to solve for the equivalent forces.
(6) When structure modifications are implemented, use equations (33) and (34) to calculate the new response of the structure.
(7) Use the resistance matrix and equation (15) to calculate the sound power radiated from the modified structure.
(8) Confirm the validity of sound power spectrum calculation by operating the structure under actual loading conditions.
(9) Steps 6–8 are repeated for multiple design changes.

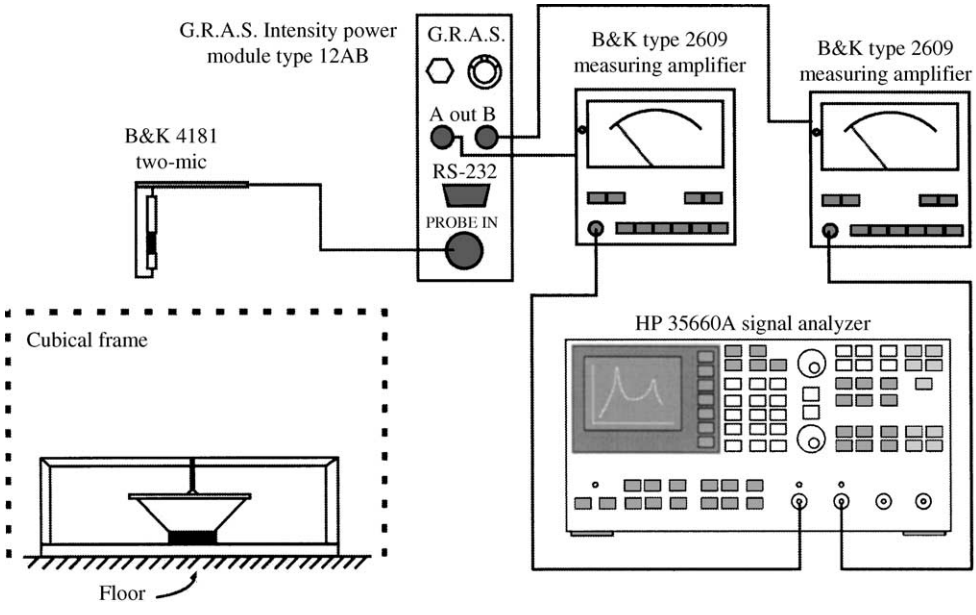

Figure 3. Experimental set-up.

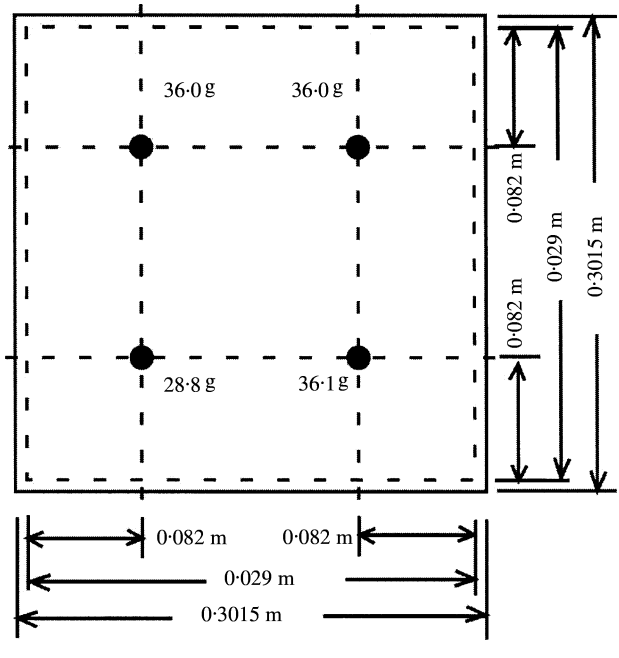

Figure 4. Aluminum plate with attached lumped masses.

4. EXPERIMENTAL MEASUREMENT OF SOUND POWER

4.1. EXPERIMENTAL SET-UP

The vibrating structure is a clamped–clamped square, cavity-backed, flat aluminum plate. The plate is 1 mm thick and the box is 88·4 mm deep. This plate is both acoustically

and structurally excited through a loudspeaker, i.e., the loudspeaker is coupled directly to the plate with a metal rod. A schematic of the experimental set-up is shown in Figure 3. A two-microphone intensity probe was used to measure the sound intensity in a semi-anechoic chamber over a surrounding rectangular surface in 1-Hz intervals. After the intensity of the unmodified plate was measured, four masses were attached and the intensity was measured again. A schematic of the mass locations is shown in Figure 4.

5. RESULTS OF EQUIVALENT FORCE EXTRACTION

The mode shapes and natural frequencies of the flat plate were computed with a MSC/NASTRAN finite element software program. Both the mode shapes and natural frequencies were confirmed experimentally, and adjustments were made to the finite element model as needed to ensure agreement. The loss factors were also determined experimentally. Figure 5 illustrates the mode shapes and Table 1 lists the natural frequencies and loss factors.

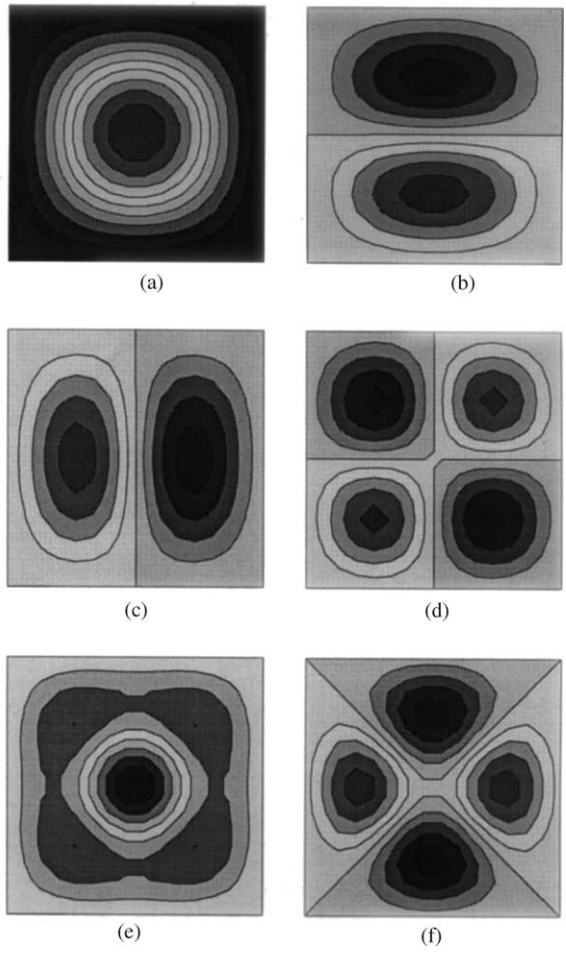

Figure 5. First six mode shapes of plate.

TABLE 1

Natural frequencies and loss factors for first six modes

Mode	Nat. freq. (Hz)	Loss factor (η)
1	132	0·033
2	225	0·029
3	234	0·029
4	317	0·026
5	333	0·025
6	384	0·022

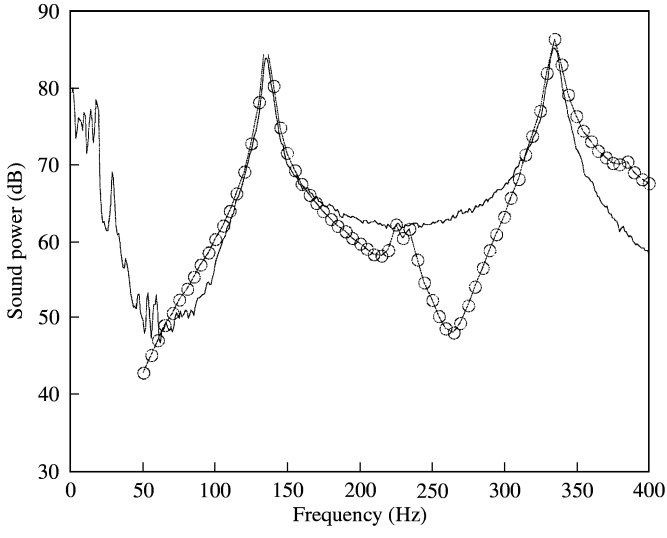

Figure 6. Experimental and analytical results for the unmodified base structure: ——, experimental; —○—, analytical.

The next step after calculating the equivalent forces was to re-calculate the radiated sound power for the unmodified structure. Figure 6 compares the original measured sound power with the sound power calculated using the equivalent force method.

Next, four masses were added, and the sound power was again measured (Figure 7). The same equivalent force used for Figure 6 was used to calculate the predicted sound power for the modified structure.

6. DISCUSSION OF RESULTS

The agreement between the analytical prediction and experimental measurement for the unmodified structure is very good, as it should be. The large difference ($\sim$ 16 dB) between the experimental and predicted sound power in a small bandwidth around 265 Hz occurs because this frequency is far from any of the structure's natural frequencies. The low structural response at this frequency results in a correspondingly low sound power output. It is important to remember that we chose to optimally match the sound power output at the natural frequencies only and thus it is not surprising that the error at frequencies far from the natural frequencies is large.

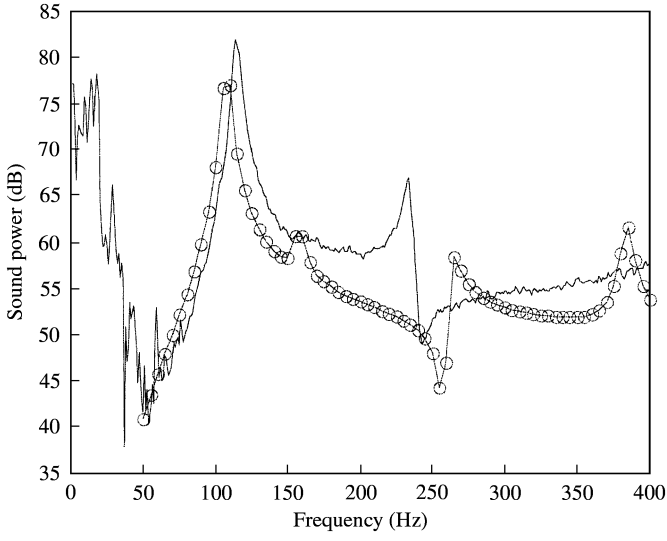

Figure 7. Experimental and analytical comparison for the modified structure: ——, experimental; —○—, analytical.

The equivalent forcing function predicts the radiated sound power of the modified structure fairly well. Most importantly, the effect of the lumped masses on the structure's resonance frequencies is predicted. A fairly small (1·5 dB) error occurs at the 105 Hz resonance peak. There is a larger error in the 150–1400 Hz frequency range, but this is acceptable because most of the radiated sound power is concentrated at the resonance peak. The peak at 386 Hz in the response of the analytical model can be explained by examining the mode shape at this frequency and the location of the masses. Figures 4 and 5(f) show that the masses lie on nodal lines. Theoretically, the masses should not have any effect on the modal response at this frequency. Recall however, that when the impedance of the lumped masses was formulated, their rotary inertia terms were neglected. The nodal lines, while having little motion normal to the surface, have significant rotary motion. Thus, if the rotary inertia terms had been included in the analytical formulation, the mode at 386 Hz would be mass-loaded, thus resulting in a reduction of sound power.

Further investigation reveals the effect the added masses had on both the experimental and analytical solutions. Experimentally, the peaks at 130 and 335 Hz moved to 110 and 225 Hz respectively. Note that the second peak has been greatly reduced in amplitude. Analytically, the peaks at 130 and 335 Hz moved to 105 and 165 Hz respectively.

It was found that the inverse method for computing equivalent forces based on sound power measurements is sensitive to how accurately the resonance frequencies of the analytical models fit those of the physical model. Small deviations between the experimental and analytical resonance frequencies result in large errors. For example, an error of 5% between the experimental and analytical resonance frequencies led to a difference of 5–6 dB in the predicted radiated sound power. Therefore, it is important to match the damped natural frequencies of the physical structure to those used in the model. To discuss the potential errors related to the matrix inversion in more quantitative terms, consider the following definitions.

For a positive-definite matrix with solution $x = A^{-1}b$, we define the *relative change* to be $\|\delta b\|/\|b\|$ and the *relative error* to be $\|\delta x\|/\|x\|$. The relative error is bounded by [19]

$$\frac{\|\delta x\|}{\|x\|} \leqslant c \frac{\|\delta b\|}{\|b\|}. \tag{35}$$

If matrix A is perturbed instead of the right side, b then [19]

$$\frac{\|\delta x\|}{\|x + \delta x\|} \leqslant c \frac{\|\delta A\|}{\|A\|}. \tag{36}$$

In the above equations, c is called the *condition number* of A. The condition number of a matrix is defined as the ratio of the largest to the smallest singular value. A matrix is *singular* if its condition number is infinite, and *ill-conditioned* if its condition number is too large, i.e., approaches the computing machine's floating point precision (10^{12} for double precision) [20]. The inverse of an ill-conditioned matrix will result in the inclusion of round-off error. Furthermore, equations (35) and (36) show that errors on the right-hand side of the equation will be amplified by an amount proportional to the condition number.

For our particular matrix (γ), the condition number is 107·9, based on the singular values of 4119·7, 3243·4, 741·2, 574·0, 82·4, and 38·2. This indicates that the matrix γ is not sufficiently ill-conditioned to cause a significant amount of round-off error. However, it should be noted that perturbation of the matrix to be inverted can also lead to errors proportional to the condition number. In this case, a condition number of 107·9 is high enough to cause significant error.

This can be explained physically. Recall that the kinetic response of a system, and therefore the acoustic response, is generally largest at resonance. By specifying an incorrect natural frequency, the method will solve for an equivalent force that satisfies a sound power value that is lower than the peak response. Therefore, the equivalent force will generally be low, which will result in an erroneously low prediction of the sound power response of the modified system. This sensitivity to resonance frequency is increased for systems that are lightly damped (i.e., those having "narrow" resonance peaks).

It is interesting to point out that good agreement between theory and experiment was obtained even though a geometrically symmetric structure with nearly degenerate modes was used. Violating the assumption that the natural frequencies be widely spaced did not have the expected adverse effect on the results for this particular case.

The next stage in this research is to validate the method with more complex impedances such as tuned vibration absorbers, stiffening ribs, and constrained layer damping treatments.

7. CONCLUSIONS

A method for computing an equivalent force for use in optimal acoustic design of structures has been derived and demonstrated for the case of a vibrating flat plate. Initially, an inverse method was developed that solved for a superposition of force distributions on a mode-by-mode basis. The solution of force distributions is based on the measurement of radiated sound power. Using radiated sound power enables us to solve for only one quantity per frequency band. The method relies on the assumption of well-separated natural frequencies and light damping to eliminate the cross terms with respect to frequency. Finally, a matrix γ is formed that includes the structural modal characteristics, control impedances, and radiation resistance matrix. The equivalent forces can be found by either inverting γ or using singular value decomposition.

Next in the procedure, the response (radiated sound power) for the plate was recalculated by representing the modifications as surface impedances. This step enables the structure response to be calculated efficiently, which is important when optimization routines are used. Point impedances in terms of lumped masses were used to validate the accuracy of the

method. Experimental results obtained by exciting a flat aluminum panel with clamped boundary conditions demonstrated that the method accurately models the effect of modifications provided that the criterion of light structural damping is met. It is generally recommended that the combination of modal density and damping gives a cross/direct term ratio of less than 0·2. It was also found that the inverse method is highly sensitive to the degree to which resonance frequencies are matched, i.e., small deviations between the experimental and analytical resonance frequencies result in large errors. This was further investigated with an analysis of the condition number of the matrix to be inverted. Therefore, it is recommended that resonance frequencies of the analytical model be "fitted" to those values determined experimentally on the physical model.

By successfully predicting the radiated sound power of a modified structure, we have demonstrated that the method presented here is feasible to use in design studies to find optimal modifications to a structure for noise control.

ACKNOWLEDGMENTS

This research was funded by the National Science Foundation Graduate Research Traineeship (NSF-GRT) Program in Environmentally Conscious Manufacturing (ECM). NSF Grant No. GRT 9454027.

REFERENCES

1. E. W. Constans, G. H. Koopmann and A. D. Belegundu 1998 *Journal of Sound and Vibration* **217**, 335–350. The use of modal tailoring to minimize the sound power of vibrating shells: theory and experiment.
2. G. Maidanik and D. W. Jordenson 1967 *Journal of the Acoustical Society of America* **42**, 494–501. Boundary wavevector filters for the study of the pressure field in a turbulent boundary layer.
3. W. K. Blake and D. M. Chase 1971 *Journal of the Acoustical Society of America* **49**, (Part 2), 862–877. Wavenumber–frequency spectra of turbulent-boundary-layer pressure measured by microphone array.
4. P. W. Jameson 1970 *Report No.* 1937 Bolt, Beranek and Newman, Inc. Measurement of low-wavenumber component of turbulent boundary layer wall pressure spectrum.
5. T. M. Farabee and F. E. Geib Jr 1975 *Paper presented at International Congress on Instrumentation in Aerospace Simulation Facilities, Ottawa, Canada.* Available as IEEE publication 75 CHO 993-6 AES, pp. 311–319 or DTNSDRC Report 76-0031. Measurement of boundary layer pressure fields with an array of pressure transducers in a subsonic flow.
6. Y. F. Hwang and F. E. Geib 1984 *Transactions of the American Society of Mechanical Engineers* **106**, 334–341. Estimation of the wavevector–frequency spectrum of turbulent boundary layer wall pressure by multiple linear regression.
7. R. A. Fulford and B. M. Gibbs 1997 *Journal of Sound and Vibration* **204**, 659–677. Structure-bourne sound power and source characterization in multi-point-connected systems. Part 1: case studies for assumed force distribution.
8. R. A. Fulford and B. M. Gibbs 1999 *Journal of Sound and Vibration* **220**, 203–224. Structure-bourne sound power and source characterization in multi-point-connected systems. Part 2: general relationships for mobility functions and free velocities.
9. R. A. Fulford and B. M. Gibbs 1999 *Journal of Sound and Vibration* **225**, 239–282. Structure-bourne sound power and source characterization in multi-point-connected systems. Part 3: force ratio estimates.
10. B. A. T. Petersson and B. M. Gibbs 1993 *Journal of Sound and Vibration* **168**, 157–176. Use of the source descriptor concept in studies of multi-point and multi-directional vibrational sources.
11. J. D. Maynard, E. G. Williams and Y. Lee 1985 *Journal of the Acoustical Society of America* **78**, 1395–1413. Nearfield acoustic holography: I. Theory of generalized holography and development of NAH.

12. W. A. VERONESI and J. D. MAYNARD 1989 *Journal of the Acoustical Society of America* **85**, 588–598. Digital holographic reconstruction of sources with arbitrarily shaped surfaces.
13. S. P. GRACE, H. M. ATASSI and W. K. BLAKE 1996 *American Institute of Aeronautics and Astronautics Journal* **34**, 2233–2240. Inverse aeroacoustic problem for a streamlined body. Part 1: basic formulation.
14. S. P. GRACE, H. M. ATASSI and W. K. BLAKE 1996 *American Institute of Aeronautics and Astronautics Journal* **34**, 2241–2246. Inverse aeroacoustic problem for a streamlined body. Part 2: accuracy of solutions.
15. P. A. NELSON and S. H. YOON 2000 *Journal of Sound and Vibration* **233**, 643–668. Estimation of acoustic source strengths by inverse methods. Part 1: conditioning of the inverse problem.
16. P. A. NELSON and S. H. YOON 2000 *Journal of Sound and Vibration* **233**, 669–705. Estimation of acoustic source strengths by inverse methods. Part 2: experimental investigation of methods for choosing regularization parameters.
17. M. A. CRAUN and D. FEIT 1999 *Proceedings of IMECE, Nashville, TN, U.S.A.* A comparison of matched-field and pseudo-inverse methods for source indentification on a frame structure.
18. E. W. CONSTANS 1998 *Ph. D. Dissertation.* Minimizing radiated sound power from vibrating shell structures: theory and experiment.
19. G. STRANG 1986 *Linear Algebra and its Applications.* San Diego: Harcourt Brace Javonovich.
20. W. H. PRESS, B. P. FLANNERY, S. A. TEUKOLSKY and W. T. VETTERLING 1989 *Numerical Recipes: The Art of Scientific Computing (FORTRAN Version).* Cambridge: Cambridge University Press.
21. G. H. KOOPMANN and J. B. FAHNLINE 1997 *Designing Quiet Structures: A Sound Power Minimization Approach.* San Diego: Academic Press, Inc.

APPENDIX A: DERIVATION OF THE ACOUSTIC RESISTANCE MATRIX

To write an expression for the radiated sound power in terms of the acoustic resistance matrix, we begin with a variation of the Kirchhoff–Helmholtz equation that uses a Green function of the second kind (rather than the more common free-space version) with the property that $\nabla_s G(x/x_s) = 0$ is satisfied on the radiating surface. The pressure is then given as

$$p(x) = -\frac{\mathrm{i}\kappa\rho c}{4\pi}\iint_S G(x/x_s)\,v(x_s)n_s\,\mathrm{d}S(x_s), \tag{A1}$$

where $p(x)$ is the pressure at the field point x (outside of the boundary surface), κ is the acoustic wave number and ρc is the characteristic acoustic impedance. The integration is taken over the radiating surface S with the integrand given as the product of the Green function G and the normal velocity of the surface $v(x_s)n_s$. To express this equation in a lumped element form, we begin by dividing the boundary surface into N elemental surfaces of area S_μ, each having a volume velocity u_ν. The space-average pressure on the element μ is

$$p(\mu) = \frac{1}{S_\mu}\iint_{S_\mu} p(x_s)\,\mathrm{d}S_\mu(x_s). \tag{A2}$$

With these approximations, the space-average pressure on element μ can be written as

$$p(\mu) \approx -\frac{\mathrm{i}\kappa\rho c}{4\pi S_\mu}\sum_\nu \frac{u(\nu)}{S_\nu}\iint_{S_\mu}\iint_{S_\nu} G(x/x_s)\,\mathrm{d}S_\nu(x_s)\,\mathrm{d}S_\mu(x). \tag{A3}$$

Taking the radiation impedance $Z^R_{\mu v}$ to be the ratio of the space-average pressure on element μ to the volume velocity source of element v, we write

$$p(\mu) = \sum_v Z^R_{\mu v}\, u(v), \tag{A4}$$

where

$$Z^R_{\mu v} = -\frac{\mathrm{i}\kappa\rho c}{4\pi S_\mu S_v} \int_{S_\mu}\int \int_{S_v}\int \{G(x/x_s)\}\, \mathrm{d}S_v(x_s)\, \mathrm{d}S_\mu(x). \tag{A5}$$

The time-average sound power radiated by a structure is

$$\Pi_{av} = \frac{1}{2}\sum_\mu \mathrm{Re}\{u^*(\mu)p(\mu)\}. \tag{A6}$$

Substituting the expression for p_μ (equation (A3)) in Π_{av}, and invoking reciprocity arguments for the impedance, i.e., $Z^R_{\mu v} = Z^R_{\mu v}$ and noting that the radiation resistance $R_{\mu v} = \mathrm{Re}\{Z^R_{\mu v}\}$, we finally write the lumped parameter approximation for the time-average sound power output as

$$\Pi_{av} = \frac{1}{2}\sum_\mu \sum_v u^*(\mu)u(v)R_{\mu v}, \tag{A7}$$

where

$$R_{\mu v} = -\frac{R_0}{S_\mu S_v} \int_{S_\mu}\int \int_{S_v}\int \mathrm{Im}\left\{\frac{G(x/x_s)}{\kappa}\right\} \mathrm{d}S(x_s)\, \mathrm{d}S(x) \tag{A8}$$

with $R_0 = \kappa^2\rho c/4\pi$.

The computer program POWER [21] is used to compute the integrals of the Green function over the elemental surfaces S_μ and S_v. POWER is an equivalent source method based on a lumped parameter model that uses volume velocity matching as a means of satisfying the boundary conditions on the surface of a radiating structure. Combinations of simple, dipole and tripole sources on each of the elemental surfaces of a structure generate volume velocities on each of those surfaces that are equivalent to the specified boundary condition. In turn, the strengths of these sources are used to calculate the space-average pressure on each elemental surface. To generate $\mathfrak{R}_{\mu 1}$, the first row of the resistance matrix, the volume velocity u_1 is unity and the volume velocity of the remaining surfaces is zero. Solution of the corresponding matrix equation yields simple, dipole and tripole source strengths that satisfy this boundary condition and are used to calculate the space-averaged surface pressure at each of the surfaces, p_μ. The full resistance matrix is computed by iterating through all of the elemental surface volume velocities in this manner. It should be noted that $\mathfrak{R}_{\mu v}$ only depends on the frequency (wavelength) of the radiated sound and the geometry of the vibrating structure.